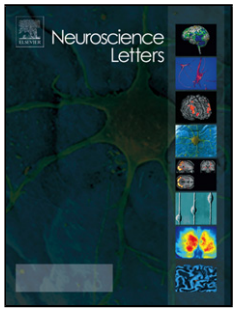

Title: CRACKING THE BARCODE OF FULLERENE-LIKE CORTICAL MICROCOLUMNS

Authors: Arturo Tozzi, James F. Peters, Ottorino Ori

PII: S0304-3940(17)30180-5
DOI: http://dx.doi.org/doi:10.1016/j.neulet.2017.02.064
Reference: NSL 32676

To appear in: *Neuroscience Letters*

Received date: 15-12-2016
Revised date: 5-2-2017
Accepted date: 22-2-2017

Please cite this article as: Arturo Tozzi, James F.Peters, Ottorino Ori, CRACKING THE BARCODE OF FULLERENE-LIKE CORTICAL MICROCOLUMNS, Neuroscience Letters http://dx.doi.org/10.1016/j.neulet.2017.02.064

CRACKING THE BARCODE OF FULLERENE-LIKE CORTICAL MICROCOLUMNS

Arturo Tozzi (corresponding Author)
Center for Nonlinear Science, University of North Texas
1155 Union Circle, #311427
Denton, TX 76203-5017, USA, and
Computational Intelligence Laboratory, University of Manitoba, Winnipeg, Canada
Winnipeg R3T 5V6 Manitoba
ASL NA2 Nord
tozziarturo@libero.it

James F. Peters
Department of Electrical and Computer Engineering, University of Manitoba
75A Chancellor's Circle, Winnipeg, MB R3T 5V6, Canada and
Department of Mathematics, Adıyaman University, 02040 Adıyaman, Turkey,
Department of Mathematics, Faculty of Arts and Sciences, Adıyaman University
02040 Adıyaman, Turkey and Computational Intelligence Laboratory, University of
Manitoba, WPG, MB, R3T 5V6, Canada
james.peters3@umanitoba.ca

Ottorino Ori
Actinium Chemical Research, Via Casilina 1626/A, 00133 Rome, Italy
ottorino.ori@gmail.com

Highlights

- Microcolumns stand for the uniform, stereotyped cortical architecture.
- Microcolumns might be arranged in guise of fullerene-like structures.
- Neural computations take place on such structures, with precise mathematical rules

ABSTRACT

Artificial neural systems and nervous graph theoretical analysis rely upon the stance that the neural code is embodied in logic circuits, *e.g.*, spatio-temporal sequences of ON/OFF spiking neurons. Nevertheless, this assumption does not fully explain complex brain functions. Here we show how nervous activity, other than logic circuits, could instead depend on topological transformations and symmetry constraints occurring at the micro-level of the cortical microcolumn, *i.e.*, the embryological, anatomical and functional basic unit of the brain. Tubular microcolumns can be flattened in fullerene-like two-dimensional lattices, equipped with about 80 nodes standing for pyramidal neurons where neural computations take place. We show how the countless possible combinations of activated neurons embedded in the lattice resemble a

barcode. Despite the fact that further experimental verification is required in order to validate our claim, different assemblies of firing neurons might have the appearance of diverse codes, each one responsible for a single mental activity. A two-dimensional fullerene-like lattice, grounded on simple topological changes standing for pyramidal neurons' activation, not just displays analogies with the real microcolumn's microcircuitry and the neural connectome, but also the potential for the manufacture of plastic, robust and fast artificial networks in robotic forms of full-fledged neural systems.

KEYWORDS:

brain circuitry; cortical neuron; neural code; lattice; artificial neural system

Current computational brain models, based on neural networks performing logic operations (Sporns 2013; Ursino et al., 2014), are not able to fully elucidate a large repertoire of brain functions and mental faculties, such as attention and perception, emotions and cognition, memory and learning, decision making and goal-directed choice (Gazzaniga, 2009), mind wandering (Andrews-Hanna et al., 2014). In order to build a versatile network able to simulate brain functions at micro-levels of observation, we introduce a cortical model, borrowed from fullerene's geometry, able to evaluate symmetry constraints and topological indices for micro-structures (Koorepazan-Moftakhar et al., 2015). Although its primary application concerns the description of carbon-networks in chemical compounds, fullerene networks can be used in order to rank topological invariants in neural networks' assessment. In particular, the method applies to description of microcolumns, i.e., the fairly uniform, stereotyped, vertical column-like architecture believed to be the basic embryological/anatomical module and the fundamental processing unit of cortical arrangement (Mountcastle 1997; Jones, 2000; Ramaswamy et al., 2015). Invariant, fullerene-like features are landmarks of microcolumnar modular connectivity. Indeed, minicolumns are characterized by translational symmetry across their central axis, rotational symmetry, transitive symmetry of morphometric relations and temporal symmetry during cortical maturation (Casanova et al., 2011; Opris and Casanova, 2014). Therefore, it is feasible to evaluate tubular microcolumns in terms of three-dimensional cylinders equipped with exagonal and pentagonal fullerenic structures. By flattening cylinders into two-dimensional rectangles, we attain lattices that make it possible for us to investigate brain microcuircuitry according to translational procedures other than ON/OFF neural firing. A fullerene-like two-dimensional sheet might be compared to a barcode, where sequences of neuronal activations stand for mental specific functions. This approach not only allows us to build a fullerene-like model that simulates the real brain, but also to assess the vibrancy and inner workings of neural computations in terms of topological relationships among firing neurons.

MATERIALS AND METHODS

Stone-Wales transformations in neural networks. Two-dimensional fullerenes are 3-regular cubic planar graphs, describable as meshes of twelve variously fused pentagons (Chuang et al., 2009; Schwerdtfeger et al., 2013; Graovac et al. 2014; Schwerdtfeger et al., 2015). Signal propagation on fullerenic networks can be investigated via graph theoretical methods. Among the possibile choices (Todeschini and Consonni, 2000), we focus on *distance-based* topological indices, able to describe long-range interactions involving all pairs of nodes. Neuronal firing and electric signal propagation are investigated in terms of pure topological network modifications. This assumption implies that the overall number of neurons (graph vertices) and connections among neurons (graph edges or bonds) are *fully preserved*, excluding neurons' creation or destruction along the process. The totally reversible topological permutations occurring on fullerene-like lattices' polygonal surfaces can be assessed and calculated. Methods based on vertex insertions or deletions and isomerisations on lattices have proven very useful, because they allow the formal derivation of one fullerene graph from another (Ori et al., 2014). In particular, the so-called Stone-Wales (SW) transformations produce a rotated figure, with no changes in fullerene's external connectivity and molecular topology outside the denoted region of the lattice surface (Babic et al., 1995). In sum, SW mechanisms extend transformations in the fullerenic mesh as a wave. They might play an important role in modifying not just the topology of carbon-based materials, like nanotubes and fullerenes (Ma et al., 2009), but also of neuronal circuits.

The general local Stone-Wales transformation $SW_{q/r}$ (**Figure 1A**) is associated with the isomeric transformation that modifies the internal connectivity of four adjacent rings with *p, q, r, s* edges, producing four new rings with *p–1,q+1,r–1,s+1* edges, leaving unchanged the surrounding lattice regions. $SW_{p/r}$ reversibly rotates the central bond bridging *p* and *r* rings, leaving unaffected both the total number of nodes $k=p+q+r+s-8$ and the total number of edges k+3. **Figures 1B-1C** illustrate the two most studied fullerenic forms, equipped with a rotation of a pentagon-hexagon double pair. SW rotations are able to generate fullerene isomers with different symmetries. In the case of the C_{60} fullerene, the *pyracylene* $SW_{5/6}$ rearrangements group the 1812 isomers in 13 inequivalent sets (**Figure 1C**). Such limitation has been solved by

using extended generalized SW transformations, in order to produce, starting from just one isomer, the whole C_{60} isomeric space (Ori et al, 2009).
Ori et al. (2011), developed a convenient graphical tool, able to modify fullerene-like networks displayed as two-dimensional graphs made by *n* vertices (*carbon atoms or neurons*), through the isomeric insertion of different *r*-rings with *r*>2. The case *r*=5,6 stands for the regular fullerene. The graphical method's efficiency relies on the dual-representation of the graph, achieved by transforming the rings in nodes, and their edges in bonds. **Figures 1D-1E** provide examples of the interplay between direct and dual representations. The graphical tool allows, as a consequence of iterated SW rotations, the identification of a peculiar topological mechanism called the Stone-Wales wave (SWw) (Ori et al, 2011), e.g., the linear migration of the pentagon-heptagon 5|7 pair in the planar network. The first $SW_{6/6}$ rotation of the connection shared by the two neurons creates two 5|7 pairs (**Figure 1D**). The second operator $SW_{6/7}$, by inserting the 6|6 couple of shaded hexagons between the two original 5|7 pairs, turns the bond between the heptagon and the shaded hexagon (**Figure 1E**). This mechanism produces the overall effect of initiating the wave propagation along the dotted direction, because iterated $SW_{6/7}$ rotations will successively propagate the topological defect 5|7. For technical details, see Koorepazan-Moftakhar, et al. (2015).

Building a fullerene-like microcolumn. Microcolumnar circuitry can be described in terms of biologically plausible fullerene-like two-dimensional lattices. A cortical microcolumn comprises 80–120 neurons, except in the primary visual cortex where the number doubles. About 80% are pyramidal neurons. This basic unit circuit forms a series of repeated items across the horizontal extent of the cortex, independent of area specializations (Jones, 2000): in humans, the transverse diameter of each of the $2x10^7$-$2x10^8$ microcolumns is about 28–50 μm (Sporns et al., 2005; Johansson and Lansner, 2007). Our knowledge of microcolumn organization is still largely incomplete, due to difficulties related to the physiological recording methods, as well as to data interpretation. However, despite few skeptical claims (Skoglund et al, 2004), several Authors (Peters and Kora, 1987, Cruz et al., 2008 Peters and Sethares, 1991, Gabbott, 2003) described microcolumnar exagonal arrangements in different cortical structures (neurons, dendritic bundles, myelinated axons packing) and in different areas and animals (monkeys, rats' area 17, human medial prefrontal cortex) and in artificial neural networks (Yoder, 2010).

According to connectomics, cortical/subcortical structures form a hierarchical network equipped with winner-takes-all mechanisms and preferential pathways for fast communication (Van den Heuvel and Sporns, 2010; Reese et al., 2012). The neural connectome is equipped with networks and energetic landscapes that can also be used for fullerene-like microcolumns' description. In the next paragraph, we will show how to build a neural network that takes into account SW connections for the 3465 isomers of the C_{64} Fullerene, using Mathematica. We will also assess fullerene-like neural networks in topological terms.

RESULTS

Here we provide simulations showing how it is feasible to generate a neural network equipped with countless alternative isomers, starting from a simple fullerene-like structure. **Figure 2A** depicts some topological transformations that might take place on microcolumns. A cortical microcolumn stands for a three-dimensional tubular armchair. By slicing at an angle to an edge, we achieve a flattened two-dimensional fullerene-like grid, a 30 microns-width lattice equipped with hexagonal (or pentagonal) tiling and about 80 nodes (**Figure 2A, left side**). Such nodes, standing for the microcortical pyramidal neurons, are linked by edges (or bonds), e.g., dendritic/axonal connections. Every node is filled with a pyramidal neuron (activated or deactivated). A preliminary activation of a pair of neurons in the 6-fold status takes place, followed by the creation of the "signal", e.g. a topological defect of the hexagonal mesh, called SW defect. Signal generation is then achieved through further rotations (**Figure 2A, right side**) that modify the local neuronal connections, by rotating the bond between the two activated elements. Additional applications of the SW operator will split more and more the neuronal pairs, allowing the signal to travel in the neural network according to the typical SWw wave mechanism.
In the nervous case, instead of SW flips on a fullerene surface, we assess changes in neuronal firing activation. Here "permutation" means which ones of the 80 pyramidal neurons are sequentially activated or deactivated. SW permutations may be regarded as a set of neurons which fire simultaneously. Every group of neural "permutations" might stand for a barcode, each one corresponding to a peculiar mental activity.
Our current lack of knowledge prevents us from assessing whether pyramidal neurons'assembly exhibits the required conformations. The Borsuk-Ulam theorem (BUT) from algebraic topology (Tozzi and Peters, 2016), helps us to solve this problem. The BUT describes antipodal points with matching description on spatial manifolds in every dimension, provided the n-sphere is a convex structure with positive curvature (*i.e.*, a ball). However, BUT can be generalized to symmetries occurring either on flat manifolds, or on Riemannian hyperbolic manifolds of concave shape (*i.e.*, a saddle)

(Mitroi-Symeonidis, 2015). Whether the system components are equipped with concave, convex, flat or "stretched" conformation, we may always find the points with matching description predicted by BUT. This means that microcolumnar's neuronal activity can always be described in terms of transformations on two-dimensional lattices, although not perfectly arranged as a sterotyped fullerene-like structure (**Figure 2B**).

We are allowed to build a 6-folded connectome-like network simulating microcolumns' behaviour. **Figure 3A** provides the SW landscape of a fullerene-like microcolumn. Every point, standing for a C_{64} fullerene isomer, is connected with the first neighbour throw a single SW rotation (of order 0). In **Figure 3A**, every single point stands for a neuronal assembly in a given configuration (say F1), while his neighbor lies in another configuration, e.g., F1 plus other faces, melted through a SW rotation. Every group is connected with others via topological deformations, depending on specific neural signals.
Figures 3B and **3C** illustrate the application of a novel topological concept, the biReBUT, on fullerenes. The details are provided in the Figure legend. This application arises from the observation of the neuronal symmetrical distribution in the left and right cortical hemispheres. That is, in brain with fullerene-like micro-structure, a pullback from each neuron to its corresponding antipodes might occur.

1) $f(A) = f(\neg A)$ for some $A \subset 2^X$
2) there is a pullback $f^{-1}(A) = f^{-1}(\neg A) = A.$

The proof of the first consequence of biReBUT is given in Peters (2016) and the second (pullback) consequence of this theorem results from the fact that the mapping f is a bijection (*i.e.*, 1-1 and onto).

DISCUSSION

We achieved a two-dimensional fullerene-like lattice reproducing microcolumn's microcircuitry. In analogy with the chess game, a fullerene network resembles a chessboard, SW transformations are analogous to moves that chess pieces can perform, and single chess pieces are the neurons. When a piece moves on the chessboard, this is analogous to a neuron firing. Our results pave the way to answer to Mountcastle's question: what are the transforming operations imposed in a cortical column, upon its input, to produce its targeted outputs (Mountcastle, 1997)? Although our lattice looks like a classical neural network at first sight, nevertheless it is faster, less energy-consuming, more plastic and stabler. It is easy to parametrize, because information can be extracted from just a few parametrizing factors. e.g., the simple topological operations taking place on networks. While other approaches emphasize macro- and meso- phenotype dynamics, our framework is grounded on operations occurring at nervous micro-levels. We assume that simultaneous firing of different neurons and specific activation sequences give rise to different topological conformations, each one corresponding to a mental activity (perception, emotion, and so on). The brain functional activity is not based on logic nodes as in conventional networks, but on topological transformations, e.g., functional changes in the firing neurons' sites.
Our model explains countless mental operations starting just from simple, stereotyped, highly preserved biological structures: the microcolumns. Fullerene-like models, involving any pair of connected nodes (Maruyama and Yamaguchi, 1998), unveil a very rich phenomenology, due to the almost infinite SW rotations that may take place. This makes possible a limitless set of moves, merely dictated by applying SW rotations on its bonds. Ubounded sets correspond to the series of mental operations taking place in our brain. During the synthesis/growth process of a C^n fullerene, the isomers with isolated pentagons often udergo SW interconversion. This may cause instability, because failures of some of its components are expected, in presence of high numbers of SW transformations. Nevertheless, the artificial implementation of the model itself grants for its stability through a simple expedient: by using a given C_n isomer as a seed, a series of moves can be performed that give us the capability to build complete sets of fullerene isomers, by simple binding topological briges (Babic et al., 1994). Therefore, both isomerization maps and complete isomer space's description can be achieved from a single known conformation. In the same way, the primal embryonal microcolumn gives rise to a huge amount of combinations in the mature individual's microcircuitry. Starting from the single vertical template of about 80 pyramidal neurons that colonizes the whole cortex during embryonal life, countless barcodes might be built with time passing. In touch with catalysts that promote fullerene transformations and stabilize its transitions states, we hypothesize that the habituation to repeated stimuli during the first months/years of life could give rise to more stable and permanent transformations in microcolumns barcodes.

Fullerene-like networks are very fast, because they use simple transformations. Starting from each randomly built C_n fullerene structure, one may directly generate a certain number of new isomers using just SW flips, instead of searching for a new one. This improves computational speed, because the number of steps required by every operation is reduced. A simple increase in the order of SW transformations allows us to connect more microcolumns: dual structures, given by the combination of many microcolumns, can be easily built by joining the reciprocal space. As nanoparticle/substrate interaction's tuning provides unique ways of controlling nanotube synthesis (Gomez-Ballesteros et al., 2015), fullerene-like neural networks might provide the fine-grain functional barcode's modularity required by different brain functions.

Fullerene-like networks take time to become efficient, because SW transformations are less favoured by an energetic standpoint. The building of novel barcodes is a slow, time-consuming process. By a biological point of view, this is in touch with the slow development of mental operations' competence in young primates (Skeide and Friederici, 2016). Vice versa, a fullerene-like neural network gives to adult primates unvaluable advantages, in terms of energy sparing. Pentagons incorporation, occurring at an early stage of nucleation pathway for single-wall nanotubes, leads to a very efficient system, because the number of dangling bonds is reduced, so that changes towards more entropic curvatures are achieved (Fan et al., 2003). To make an example, fullerenes produced by the overlap of 12 nanocones which no direct pentagon fusion display very high thermodynamic stability, steady topological configurations and minimized graph invariants (Vukicevic et al., 2011; Ori et al., 2014). In mental terms, a fullerene-like microcolumnar structure might be associated with minimal wiring costs and fast synchronization/information transfer (Stam and Reijneveld, 2007).

The concept of nervous connectome might be extended not just to the "classical" macro and meso- levels, but also to the microcolumnar level. Our observations suggest that connectome's nodes, hubs, energetic fluxes and trajectory paths are diffused along the entire neural pathway, including microcolumnar arrangement. This is in touch with the recently described micro-commectome, i.e., neural netwoks at cellular scale (Schröter et al., 2017).

In terms of age-related mental decline and of a broad spectrum of neurologic and psychiatric disorders (autism, schizophrenia, Alzheimer disease, drug addiction), the results so far available point towards a loss of regularity and changes in the structural coherence of the microcolumnar organization and/or connectome modularity (Cruz et al., 2009; Opris and Casanova, 2014). These features could be assessed in term of fullerene-like microcolumns. Indeed, defects of graphene nucleation/growth modify physical/chemical features of carbon nanostructures, generating lattice functional failures (Hashimoto et al., 2004).

In sum, we make available a novel approach that allows us to evaluate topological brain activity in terms of fullerenes' graph properties. This powerful method could be, in a near future, applied to the assessment of neural networks, in order to achieve a double task: improving our understanding of biological brain function in situ, and building computers that simulate cortical activities. We would like to bring to an end with a methodological remark. Once high density neurotechniques will be able of capturing the simultaneous activity of larger populations (Koster et al., 2014), we suggest to analyize microcolumnar activity in primate temporal cortex or other associative cortices (instead of the "classical" rodents' barrel cortex or primates' visual cortex), because they display a notable sterotypy (Jones, 2000), which may prove to be a better model.

REFERENCES

1. Andrews-Hanna JR, Smallwood J, Spreng RN. 2014. The default network and self-generated thought: component processes, dynamic control, and clinical relevance. Ann. N. Y. Acad. Sci. 1316, 29-52.
2. Babic D, Bassoli S, Casartelli M, Cataldo F, Graovac A, et al. 1995. Generalized Stone-Whales transformations. Molecular Simulation, 14, 395-401.
3. Blagojevic PVM, Ziegler GM. 2016. Beyond the Borsuk-Ulam theorem: The topological Tverberg story, arXiv 1605.07321, 1-34.
4. Buxhoeveden DP, Casanova MF. 2002. The minicolumn hypothesis in neuroscience. Brain, 125, 5:935–951.
5. Casanova MF, El-Baz A, Switala A. 2011. Laws of conservation as related to brain growth, aging, and evolution: symmetry of the minicolumn. Front Neuroanat. 26;5:66. doi: 10.3389/fnana.2011.00066.
6. Chuang C, Fan Y-C and Jin B-J. 2009. Generalized Classification Scheme of Toroidal and Helical Carbon Nanotubes. J. Chem. Inf. Model., 2009, 49 (2), pp 361–368. DOI: 10.1021/ci800395r.
7. Cruz L, Urbanc B, Inglis A, Rosene DL, Stanley HE. 2008. Generating a model of the Three-dimensional Spatial Distribution of Neurons using Density Maps. Neuroimage. 40(3): 1105–1115.
8. Cruz L, Roe DL, Urbanc B, Inglis A, Stanley HE, Rosene DL. 2009. Age-related reduction in microcolumnar structure correlates with cognitive decline in ventral but not dorsal area 46 of the rhesus monkey. Neuroscience. 18;158(4):1509-20.
9. Fan X, Buczko R, Puretzky AA, Geohegan DB, Howe JY, Pantelides ST, Pennycook SJ. 2003. Nucleation of Single-Walled Carbon Nanotubes. Phys. Rev. Lett. 90, 145501.
10. Gabbott PLA. 2003. Radial organization of neurons and dendrites in human cortical areas 25, 32, and 32′ Brain Research. 992:298–304.
11. Gazzaniga MS. 2009. The Cognitive Neurosciences, Fourth Edition. MIT Press. ISBN: 9780262013413
12. Gomez-Ballesteros JL, Burgos JC, Lin PA, Sharma R, Balbuena PB. 2015. Nanocatalyst shape and composition during nucleation of single-walled carbon nanotubes. RSC Adv. 5(129): 106377–106386. doi: 10.1039/C5RA21877B.
13. Graovac A, Ashrafi AR, Ori O. 2014. Topological Efficiency Approach to Fullerene Stability – Case Study with C50. Advances in Mathematical Chemistry and Applications, 2: 3-23. Subash C. Basak, Guillermo Restrepo& Jose L. Villaveces (Eds) Bentham Science Publishers.
14. Hashimoto A, Suenaga K, Gloter A, Urita K, Iijima S. 2004. Direct evidence for atomic defects in graphene layers. Nature, 19;430(7002):870-3.
15. Johansson C, Lansner A. 2007. Towards cortex sized artificial neural systems. Neural Networks, Vol. 20 #1, 48–61, Elsevier.
16. Jones EG. 2000. Microcolumns in the cerebral cortex. PNAS, 97 10:5019-5021. doi:10.1073/pnas.97.10.5019
17. Koorepazan-Moftakhar F, Ashrafi AR, Ori O, Putz MV. 2015. Geometry and Topology of Nanotubes and Nanotori. Exotic Properties of Carbon Nanomatter. Volume 8 of the series Carbon Materials: Chemistry and Physics pp 131-152
18. Köster U, Sohl-Dickstein J, Gray CM, Olshausen BA. 2014. Modeling Higher-Order Correlations within Cortical Microcolumns. PLoSComputBiol, 10(7): e1003684.
19. Ma J, Alfè D, Michaelides A, Wang E. 2009. Stone-Wales defects in graphene and other planar sp2-bonded materials. Physical Review B 80, 033407.
20. Maruyama S, Yamaguchi Y. 1998. A molecular dynamics demonstration of annealing to a perfect C60 structure. Chemical Physics Letters, 286, Issues 3–4, 343–349.
21. Mitroi-Symeonidis F-C. 2015. Convexity and sandwich theorems. European Journal of Research in Applied Sciences, vol. 1: 9-11
22. Mountcastle VB. 1997. The columnar organization of the neocortex. Brain, 20, 4: 701–722.
23. Opris I, Casanova MF. 2014. Prefrontal cortical minicolumn: from executive control to disrupted cognitive processing. Brain. 2014 Jul;137(Pt 7):1863-75. doi: 10.1093/brain/awt359.
24. Ori O, Cataldo F, Graovac A. 2009. Topological Ranking of C28 Fullerenes Reactivity. Fullerenes, Nanotubes and Carbon Nanostructures,17:3,308 — 323. DOI: 10.1080/15363830902782332.
25. Ori O, Cataldo F, Putz MV. 2011. Topological Anisotropy of Stone-Wales Waves in Graphenic Fragments. Int. J. Mol. Sci. 12:7934-7949; doi:10.3390/ijms12117934.
26. Ori O, Putz MV, Gutman I, Schwerdtfeger P. 2014. Generalized Stone-Wales Transformations for Fullerene Graphs Derived from Berge's Switching Theorem. Ante Graovac — Life and Works. Gutman I, Pokric B, Vukicevic D (Eds.), 259-272.
27. Peters, J.F. 2016. Computational Proximity. Excursions in the Topology of Digital Images. Intelligent Systems Reference Library. Berlin: Springer-Verlag. doi:10.1007/978-3-319-30262-1.
28. Peters JF, Tozzi A. 2016. Region-Based Borsuk-Ulam Theorem. arXiv.1605.02987.
29. Peters A, Kara DA. 1987. Neuronal composition of area 17 of rat visual cortex. iv. the organization of pyramidal cells. The Journal of Comparative Neurology. 260(4):573–590.

30. Peters A, Sethares C. 1991. Organization of pyramidal neurons in area-17 of monkey visual-cortex. Journal of Comparative Neurology. 1991;306(1):1–23.
31. Ramaswamy S, Courcol JD, Abdellah M, Adaszewski SR, Antille N, et al. 2015. The neocortical microcircuit collaboration portal: a resource for rat somatosensory cortex. Front Neural Circuits. 9:44. doi: 10.3389/fncir.2015.00044. eCollection 2015.
32. Reese TM, Brzoska A, Yott DT, Kelleher DJ. 2012 Analyzing Self-Similar and Fractal Properties of the C. elegans Neural Network. PLoS ONE 7,(10): e40483. (doi:10.1371/journal.pone.0040483).
33. Schröter M, Paulsen O, Bullmore ET. 2017. Micro-connectomics: probing the organization of neuronal networks at the cellular scale. Nat Rev Neurosci. doi: 10.1038/nrn.2016.182.
34. Schwerdtfeger P, WirzL, Avery J. 2013. J Comput Chem, 34, 1508-1526.
35. Schwerdtfeger P, Wirz L, Avery J. 2015. The Topology of Fullerenes. Wiley Interdisciplinary Reviews: Computational Molecular Science 5, 96-145.
36. Skeide MA, Friederici AD. 2016. The ontogeny of the cortical language network. Nature ReviewsNeuroscience 17, 323–332. doi:10.1038/nrn.2016.23.
37. Skoglund TS, Pascher R, Berthold CH. 2004. Aspects of the organization of neurons and dendritic bundles in primary somatosensory cortex of the rat. Neuroscience Research. 50(2):189–198.
38. Sporns O, Tononi G, Kötter R. 2005. The human connectome: A structural description of the human brain. PLoSComput. Biol. 1(4):e42.
39. Sporns O. 2013. Structure and function of complex brain networks. Dialogues ClinNeurosci. 2013 Sep; 15(3): 247–262.
40. Stam CJ, Reijneveld JC. 2007. Graph theoretical analysis of complex networks in the brain. Nonlinear Biomed Phys, 5; 1(1):3.
41. Todeschini R, Consonni V. 2000. Handbook of Molecular Descriptors. Wiley-VCH: Weinheim, Germany.
42. Tozzi A, Peters JF. 2016. A Topological Approach Unveils System Invariances and Broken Symmetries in the Brain. Journal of Neuroscience Research 94 (5): 351–65. doi:10.1002/jnr.23720.
43. Ursino M, Cuppini C, Magosso E. 2014. A neural network for learning the meaning of objects and words from a featural representation. Neural Networks 63. DOI: 10.1016/j.neunet.2014.11.009.
44. Van den Heuvel MP, Sporns O. 2011. Rich-club organization of the human connectome. J Neurosci. 2;31(44):15775-86.
45. Vukicevic D, Cataldo F, Ori O, Graovac A. 2011. Topological efficiency of C66 fullerene. Chemical Physics Letters, 501, 4–6: 442–445.
46. Yoder L. 2010. Explicit logic circuits predict local properties of the neocortex's physiology and anatomy. PLoS One. 5(2):e9227. doi: 10.1371/journal.pone.0009227.

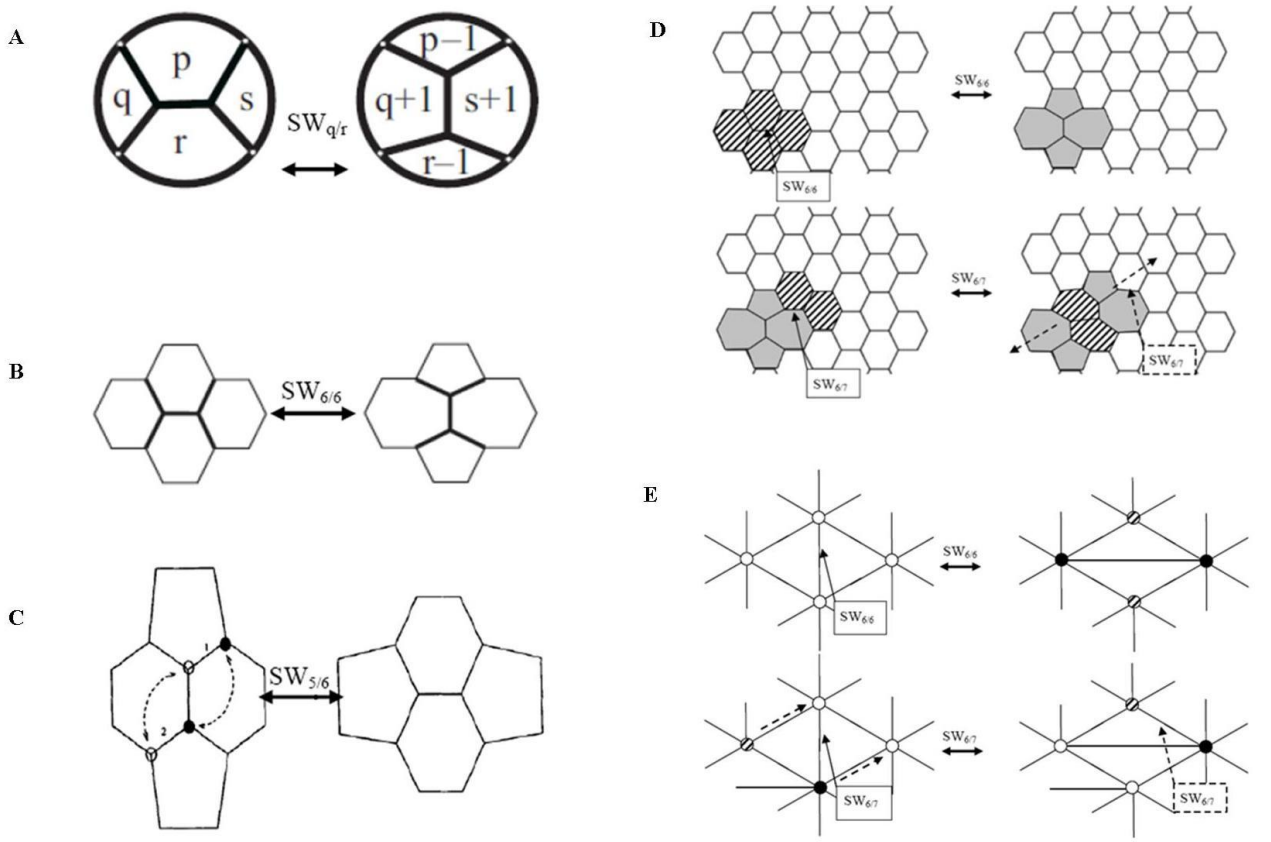

Figures 1A-1C. Examples of Stone-Wales transformation $SW_{q/r.}$ **Figure 1A**: the general $SW_{q/r}$ rotation reversibly transforms four proximal polygons with p, q, r, s edges in four new rings with p–1, q+1, r–1, s+1 nodes. **Figure 1B**: in the graphene p=q=r=s=6, which stands for the $SW_{6/6}$ rotation normally encountered in carbon nanotubes, $SW_{6/6}$ flips four hexagons in a 5|7 double pair. **Figure 1C**: the so-called "pyracylene rearrangement $SW_{5/6}$" displays a $SW_{5/6}$ rotation. **Figures 1D-E** summarize the basic topological operations for generating and propagating SWw in lattices. **Figure 1D**: in the direct graph, $SW_{6/6}$ originates two 5|7 pairs (gray), then $SW_{6/7}$ splits them, by swapping one of the 5|7 two pairs with a pair of hexagons (shaded); the dotted $SW_{6/7}$ propagates the SW wave in the dashed direction. **Figure 1E** illustrates the same transformations in the dual plane. Hexagons, pentagons, heptagons are displayed by white, shaded, black circles respectively.

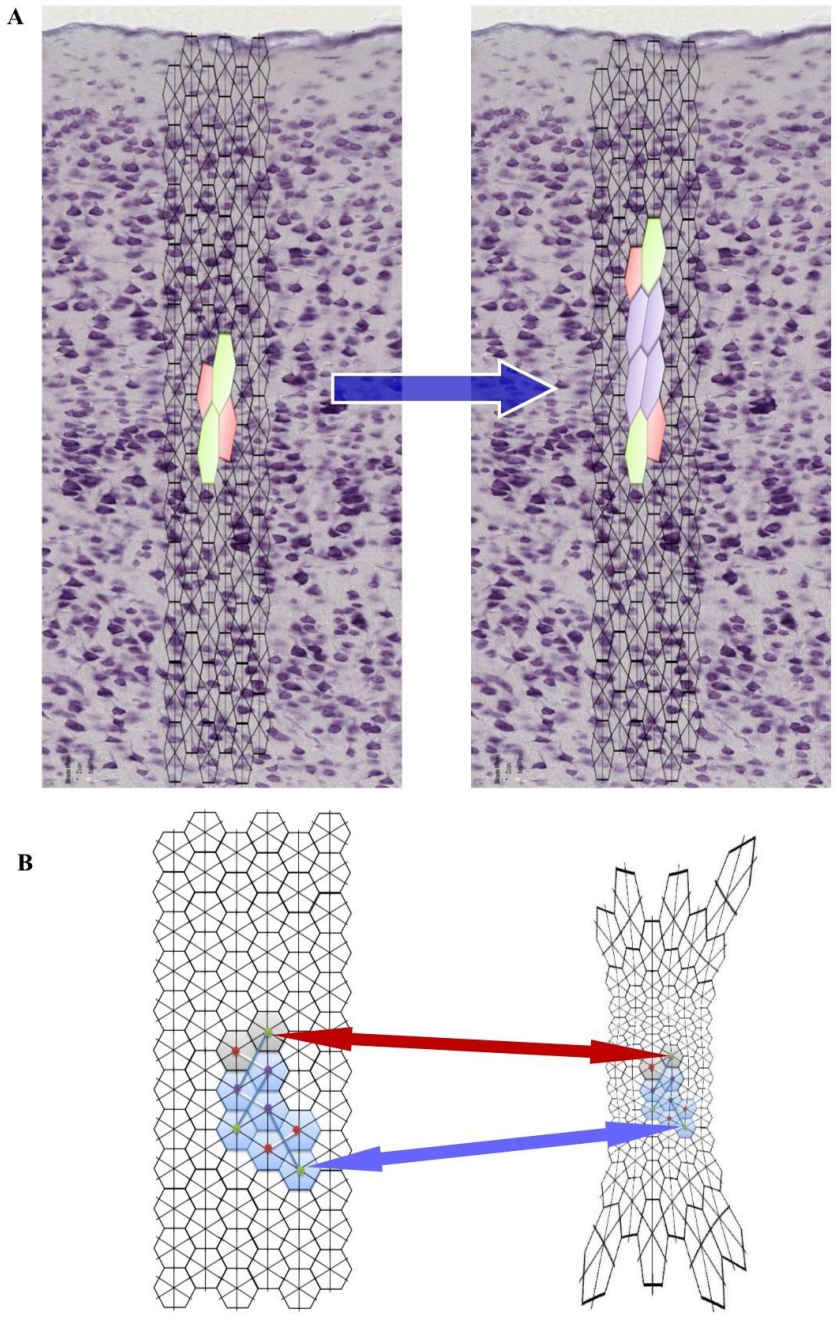

Figure 2A. Topological simulation of propagating signals on a fullerene-like grid, embedded in situ into a cortical micrococolumn. The stained exagons, depicting SW transformations in lattice's nodes, stand for activated pyramidal neurons. In this example, the flat hexagonal lattice, equipped with 72 nodes, 6-bonds each, stands for a cortical microcolumn containing 72 pyramidal neurons. Starting from the totally inactive state of 6-fold nodes on 6x12 lattice, some nodes (neurons) get activated (**Figure 2A, left side**). We may select whatever pair in the mesh. In **Figure 2A, right side**, signal propagation gives rise to a sequential activation of novel front nodes: the waves propagate steps further. **Figure 2B**. Every deformation in fullerene-like lattices leaves the relationships among the single elements (the firing neurons) unchanged, due to the BUT dictates.

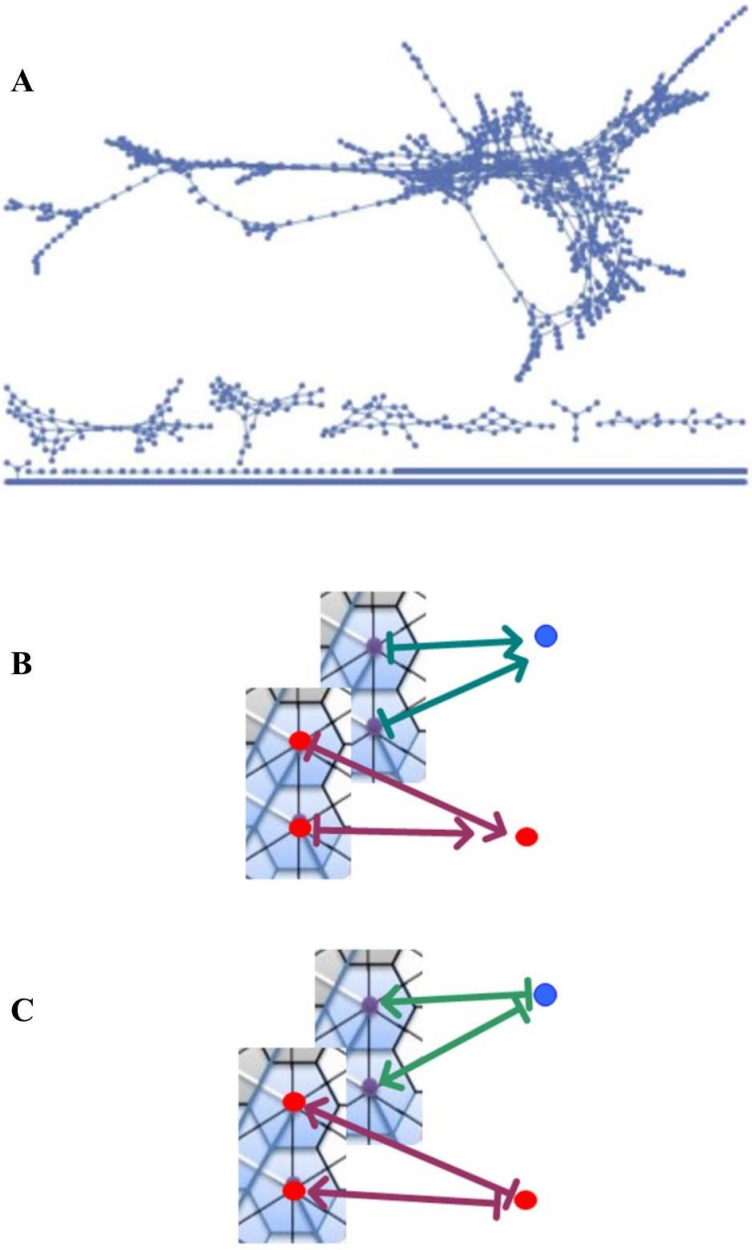

Figure 3A. Topological ranking of C_{64} isomers landscape. Signals can be connected by one up to 4 SW rotations. Here we provide, as an example, the graph defining the isomers that are connected by SW transformations of order G0 (i.e., a single SW rotation). Other graphs of different orders (G1, G2, G3) can be built.

Figure 3B. Region-based BUT (reBUT) results in a mapping of matching pyramidal neurons with matching descriptions (on a brain emisphere) to a single neuronal region ● (on the other emisphere). The neurons with matching description stand for activated neurons. reBUT comes into play by observing fullerene pyramidal neuronal regions with matching descriptions, and mapping the observed fullerene regions to a corresponding neuron in the other emisphere. For more about reBUT, see Peters (2016) and Peters, Tozzi (2016).

Figure 3C. The bijective version of reBUT (**biReBUT**) states that if $f : 2^X \rightarrow 2^{R^k}$ is a continuous bijection from a collection of regions 2^X onto a collection of planar vectors 2^{R^k} in a *k*-dimensional space R^k, then: